



Effects of Re- and Al-alloying on mechanical properties and high-temperature oxidation of MoSi₂

A.A. Sharif*

California State University Los Angeles, Department of Mechanical Engineering 5151 State University Dr., Los Angeles, CA 90032-8153, USA

ARTICLE INFO

Article history:

Received 5 December 2009
Received in revised form
17 December 2011
Accepted 19 December 2011
Available online 27 December 2011

Keywords:

High-temperature alloys
Intermetallics
Oxidation

ABSTRACT

Alloying with Re and Al improves high-temperature strength and low-temperature ductility of MoSi₂, respectively. The effects of Re + Al on strength and ductility of MoSi₂ is the combination of their individual effects, resulting in an alloy whose BDTT is lowered to room temperature and whose strength at 1600 °C is enhanced by better than one order of magnitude. However, the effects of these alloying elements on oxidation resistance of MoSi₂ were not as promising as the effects on mechanical properties. Alloying with 2 at% Al resulted in acceleration of the oxidation rate of MoSi₂ by about one order of magnitude, whereas alloying with 1 at% Re had little or no effect on oxidation rate at 1400–1700 °C. Moreover, alloying MoSi₂ with 1 at% Re + 2 at% Al resulted in deterioration of the high-temperature oxidation resistance of MoSi₂ beyond the effects of Al alone.

© 2011 Elsevier B.V. All rights reserved.

1. Introduction

Molybdenum disilicide (MoSi₂) -based alloys are materials potentially capable of replacing Ni-based superalloys to increase the operating temperature of gas engines and to enhance their efficiencies. Problems with pest oxidation, low-temperature brittleness, insufficient high-temperature strength, and oxide scale spallation have hindered development of MoSi₂-based alloys for applications as high-temperature structural materials. Recent advances have shown that pest oxidation may be overcome by alloying and processing techniques [1,2], and both low-temperature ductility and high-temperature strength may be improved by alloying [3–5]. Presence of secondary phases has also shown to improve ductility of MoSi₂-based alloys. For instance, an increase of more than 20% in the fracture toughness was observed in MoSi₂/NbSi₂ duplex specimens [6]. However, alloying in general results in degradation of oxidation resistance of MoSi₂ and may cause spallation of the oxide layer, whose integrity is essential for high-temperature stability of the material.

Enhanced low-temperature ductility in Al-alloyed MoSi₂ has been reported by several investigators [4,7–11]. Previous investigations have indicated that the brittle to ductile transition temperature (BDTT) of MoSi₂ may be lowered from ~900 °C to 25 °C by alloying with 2 at% Al [12]. Inui et al. [4] determined that the addition of 1.5 at% Al lowered the yield strength of MoSi₂ in

the temperature range of 25–1500 °C. Harada et al. [11] found that addition of 0.5 at% Al to MoSi₂ decreased Vickers hardness from 25 °C to 1200 °C, whereas alloying with 1 at% Al increased Vickers hardness above 600 °C. While improving its ductility and pest resistance [7], Al impurity lowers the high-temperature oxidation resistance of MoSi₂ [13–15]. However, as the fraction of Al in the alloy is increased above the solubility limit in the tetragonal MoSi₂, formation of an alumina (Al₂O₃) and/or mullite (2SiO₂·3Al₂O₃) [16] may result in an improved oxidation resistance [15].

Significant solid solution hardening has been observed by alloying MoSi₂ with small amounts, <2.5 at%, of Re at all temperatures [4,11]. Misra et al. observed remarkable improvements in high-temperature (1200–1600 °C) mechanical properties of MoSi₂ by alloying with 2.5 at% Re. Inui et al. [9] determined that alloying single crystals of MoSi₂ with 1 at% Re had the same hardening effect as 17 at% W at the temperature range of 1300–1500 °C. However, the effects of Re and Re + Al alloying on oxidation resistance of MoSi₂ are unknown.

MoSi₂ exhibits a complex oxidation behavior. It undergoes pest oxidation at the temperature range of ~500–800 °C; its oxidation reaction produces volatile products at low temperatures; and it forms an excellent protective oxide layer at high temperatures, typical of all SiO₂-forming materials. Oxidation rates and controlling mechanisms change with increasing temperature, which includes surface reaction, pesting, volatilization of Mo oxides, formation of Mo₅Si₃ phase, and formation of SiO₂ scale [17,18]. It is only at temperatures about 1400 °C that formation of a stable protective scale occurs in unalloyed MoSi₂ [18].

* Tel.: +1 323 343 4478; fax: +1 323 343 5004.
E-mail address: aasharif@calstatela.edu

Varying amounts of different alloying elements distinctly affect pesting, volatilization, and scale formation during oxidation of MoSi_2 . Impurities may influence the rate-controlling mechanism for oxidation or may affect the adhesion of the oxide scale to the sample surface. Furthermore, in addition to SiO_2 , other oxides, as well as silicides of molybdenum, may be present during oxidation of MoSi_2 . It is not unusual for several different phases to form on the sample surface during oxidation. The formation or absence of each phase that develops during oxidation may have a beneficial or a deleterious effect on oxidation resistance. Since each alloying element may influence formation of various phases, it is important to investigate the effects of alloying elements on oxidation resistance of MoSi_2 along with the investigations of their effects on mechanical properties. Furthermore, the combined effects of the impurities should be investigated if more than one impurity element is to be used in the same alloy. It is the aim of the present study to investigate the effects of alloying elements Re, Al, and Re + Al on low-temperature ductility, high-temperature strength, and high-temperature oxidation resistance of MoSi_2 .

2. Experimental procedures

Polycrystalline MoSi_2 buttons were prepared by arc-melting elemental Mo with 99.95% purity, Si with 99.999% purity, Al with 99.999% purity, and Re with 99.99% purity in an argon atmosphere. Excess Si in the amount of 0.1 at% was added to all samples to compensate for the Si loss that occurs during arc-melting. During arc-melting, each sample was turned over and re-melted four times to ensure homogeneity. For compression testing, parallelepiped samples with dimensions of $2\text{ mm} \times 2\text{ mm} \times 4\text{ mm}$ were sectioned from the arc-melted alloys. After polishing the samples down to $0.05\text{ }\mu\text{m}$, they were cleaned ultrasonically and placed between alumina platens for compression testing in air from $25\text{ }^\circ\text{C}$ to $1600\text{ }^\circ\text{C}$ at a strain rate of about 10^{-4} s^{-1} . Unalloyed MoSi_2 samples would not deform plastically below $900\text{ }^\circ\text{C}$. Yield strengths for polycrystalline samples below $900\text{ }^\circ\text{C}$ were estimated from results of compression testing of single crystals.

For oxidation testing, the as-melted buttons with a base diameter of about 11 mm and height of about 6 mm were used without polishing to eliminate introduction of microcracks during cutting and polishing. The surface area of the samples was estimated by calculating areas of the strips that would be obtained by cutting disks parallel to the base of the droplet and opening these disks to obtain trapezoidal surfaces. These samples were cleaned ultrasonically in methanol and weighed using a microbalance after drying. The samples were placed in an air-furnace at designated temperatures and were allowed to oxidize for 3, 13, 25, 50, 75, and 100 h. Furnace heating and cooling rate was about $25\text{ }^\circ\text{C}/\text{min}$. After each oxidation interval, the samples were weighed and returned to the furnace. Upon completion of 100 h of oxidation, samples were sectioned and polished on one side to remove the oxide layer and to expose the cross section of the oxide layer on the other sides. Oxide thickness measurements were performed on micrographs of the cross section of the oxide scale obtained by scanning electron microscopy (SEM). Composition of the phases present was determined by energy-dispersive X-ray spectrometer (EDS). X-ray analysis for determining MoSi_2 crystal structure is published previously [19].

3. Results and discussion

Preparation of MoSi_2 by arc-melting results in vaporization of some Si, which results in a Si-deficient alloy instead of a stoichiometric composition. Si vaporization resulted in formation of a Mo-rich phase, i.e., Mo_5Si_3 , which was observed as bright veins at the grain boundaries of MoSi_2 in the BSE image shown in Fig. 1a. However, addition of 0.2 at% Si in excess of stoichiometry resulted in samples with grain boundary rich in Si as seen in Fig. 1c. The faint veins of Fig. 1c were not ubiquitously present throughout the samples and are shown here to indicate the variability of the composition in the samples. A nearly stoichiometric alloy was obtained in samples with starting composition of 0.1 at% excess Si, as seen in Fig. 1b. The starting compositions for alloys depicted in Fig. 1a, b, and c for 1 at% Re + 2 at% Al containing samples correspond to $(\text{Mo}_{0.97}\text{Re}_{0.03})(\text{Si}_{0.97}\text{Al}_{0.03})_2$, $(\text{Mo}_{0.97}\text{Re}_{0.03})(\text{Si}_{0.975}\text{Al}_{0.03})_2$, and $(\text{Mo}_{0.97}\text{Re}_{0.03})(\text{Si}_{0.98}\text{Al}_{0.03})_2$, respectively. Henceforth, when we refer to MoSi_2 and its alloys, we will be referring to alloys with premelt composition of 0.1 at% excess Si.

3.1. Mechanical properties

Compilation of yield strengths of samples as a function of temperature is shown in Fig. 2. Unalloyed polycrystalline MoSi_2 does not undergo plastic deformation below $900\text{ }^\circ\text{C}$. Yield strengths of polycrystalline samples below $900\text{ }^\circ\text{C}$ were estimated from the critical resolved shear stress (CRSS) of the operative slip systems in single crystals. Pure MoSi_2 exhibited a moderate strength of 276 MPa above its BDTT at $900\text{ }^\circ\text{C}$, but its yield strength decreased rapidly to 14 MPa by increasing the temperature to $1600\text{ }^\circ\text{C}$. However, addition of 2.5 at% Re to MoSi_2 resulted in elevating its BDTT from $\sim 900\text{ }^\circ\text{C}$ to $\sim 1200\text{ }^\circ\text{C}$. At higher temperatures, the effect of 2.5 at% Re on yield strength of MoSi_2 was significant, raising it to 170 MPa at $1600\text{ }^\circ\text{C}$. This anomalously high hardening effect of Re on MoSi_2 may not be explained by the solution hardening effect that results from shear modulus mismatch and atomic size misfit described by the Fleischer model [20]. Since molybdenum “disilicide” has a Si-deficient stoichiometry of Re_4Si_7 [21], it can be shown that every four Re impurity atoms results in one Si vacancy in MoSi_2 . Pairing of point defects creates defect complexes with large strain fields whose interaction with dislocations results in a significantly higher hardening rate than the classic hardening expected from substitutional Re defects.

The effects of alloying with 2.0 at% Al on the strength of MoSi_2 is insignificant above $800\text{ }^\circ\text{C}$. However, at low temperatures, 2.0 at% Al alloying resulted in significant improvements in low-temperature

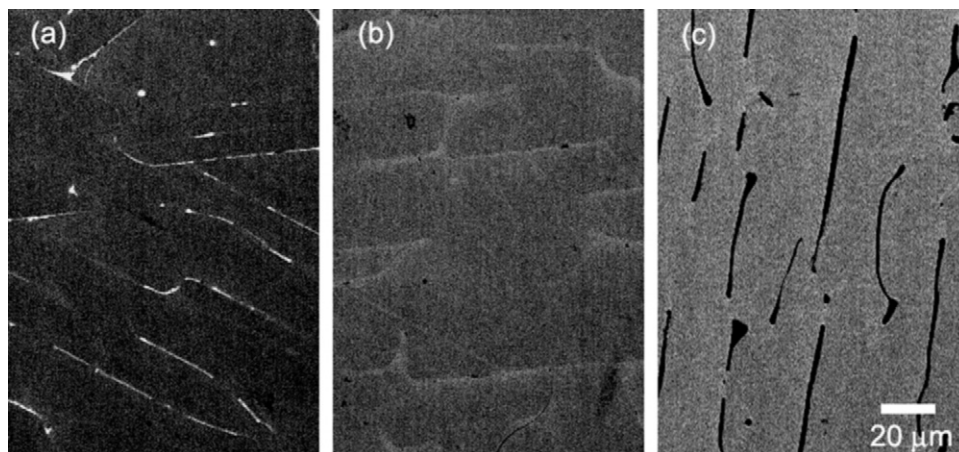


Fig. 1. Back-scatter electron images of $\text{MoSi}_2 + 1\text{ at}\% \text{ Re} + 2\text{ at}\% \text{ Al}$ alloys after arc-melting (A) $(\text{Mo}_{0.97}\text{Re}_{0.03})(\text{Si}_{0.97}\text{Al}_{0.03})_2$, showing a Si-deficient sample, (B) $(\text{Mo}_{0.97}\text{Re}_{0.03})(\text{Si}_{0.975}\text{Al}_{0.03})_2$, showing a stoichiometric sample composition, and (C) $(\text{Mo}_{0.97}\text{Re}_{0.03})(\text{Si}_{0.98}\text{Al}_{0.03})_2$, showing a Si-rich sample.

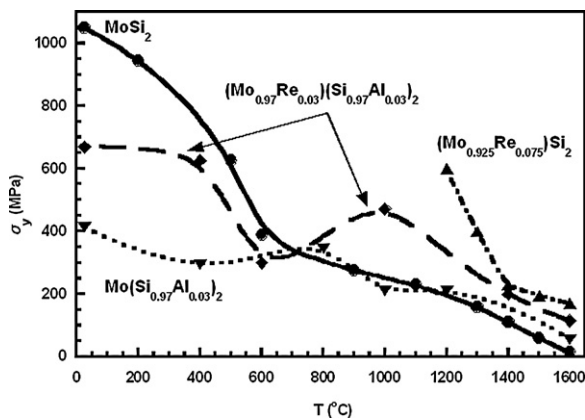


Fig. 2. 0.2% offset yield strength from 25 to 1600 °C for MoSi₂ samples containing 2.5 at% Re, 2.0 at% Al, and 1.0 at% Re + 2.0 at% Al. Yield strength of unalloyed MoSi₂ at the temperature range of 25–900 °C was estimated from the single crystal data.

ductility, lowering the BDTT to ≤ 25 °C. Yield strength of unalloyed MoSi₂ calculated from the single crystal CRSS at 25 °C is 1050 MPa. Addition of 2.0 at% Al to MoSi₂ decreased the ambient-temperature yield strength to 415 MPa. Alloying of MoSi₂ with Al beyond its solubility limit in tetragonal C11_b structure [16] results in changing the structure to hexagonal C40. These two structures of MoSi₂ are closely related signified by the c/a ratio of the C11_b structure, which is about $\sqrt{6}$. Al-alloying stabilizes the stacking sequence of the hexagonal structure relative to that of the tetragonal structure resulting in a decrease in the stacking fault energy of the $1/4(111)$ partial dislocations on $\{110\}$ [22]. This lowering of the stacking fault energy and thereby increasing the width of the faulted region affects the Peierls stress and dislocation mobility and results in enhanced ductility.

Within their solubility limits in MoSi₂, Re substitutes for Mo, and Al substitutes for Si. Because Al and Re do not react to form an Al–Re phase, the combined effect of Al and Re solutes on strength at low and high temperatures becomes the sum of the effects of individual elements. The only Al–Re phase that could possibly increase the high-temperature strength of MoSi₂ would be AlRe₂, which has a melting temperature of ~ 2000 °C \pm 25 °C [23]; all other intermetallic compounds of Al and Re have melting temperatures lower than 1590 °C, and their presence would result in the softening of MoSi₂ at high temperatures. If AlRe₂ were to form, its effect on hardening would result in a degree of hardening comparable to that which is expected from precipitate hardening above 1590 °C, and solution softening at low temperatures would not be observed. Formation of AlRe₂ may be excluded, however, since hardening by the combined effects of Al and Re is much greater than precipitate hardening at high temperatures and is accompanied by softening at low temperatures. Other Al and Re compounds may also be excluded as they would not result in solution hardening at high temperatures. Therefore, both solid solution softening and hardening effects observed here are caused by elemental Al and Re impurities.

Alloying with 1 at% Re + 2 at% Al seems to give MoSi₂ the benefits of alloying individually with these elements. The (Mo_{0.97}–Re_{0.03})(Si_{0.97}–Al_{0.03})₂ alloy retained most of the low-temperature ductility that was obtained by Al-alloying alone and most of the high-temperature strengthening obtained by Re-alloying alone. The effect of 1 at% Re on hardening rate was less than that observed in samples containing 2.5 at% Re. This was expected as the number of defect complexes that would interact with dislocation to strengthen the alloy decreases by decreasing the amount of Re in the alloy. At 1600 °C, yield strength of the samples with 1 at% Re + 2 at% Al was 115 MPa, markedly higher than 14 MPa for the unalloyed sample. However, at low temperatures, it seems that

solution hardening by Re nullified some of the beneficial effects of solution softening caused by Al. At 25 °C the yield strength of the 1 at% Re + 2 at% Al containing sample was 670 MPa. Although significantly lower than 1050 MPa for the pure sample, it is higher than 415 MPa for the samples that contained only Al.

3.2. Oxidation behavior

Cross sections of the samples after 100 h of oxidation at 1700 °C are shown in Fig. 3 for (A) unalloyed MoSi₂, (B) MoSi₂ + 2 at% Al, (C) MoSi₂ + 1 at% Re, and (D) MoSi₂ + 1 at% Re + 2 at% Al. The three regions observed in the cross sections are the silica (SiO₂) scale, a layer of Mo₅Si₃, and the bulk MoSi₂. The Mo-rich Mo₅Si₃ phase is formed as a result of rapid Si consumption during oxidation at high temperatures [19], and its thickness varies depending on the alloying elements. After 100 h at 1700 °C, the Mo₅Si₃ phase was about

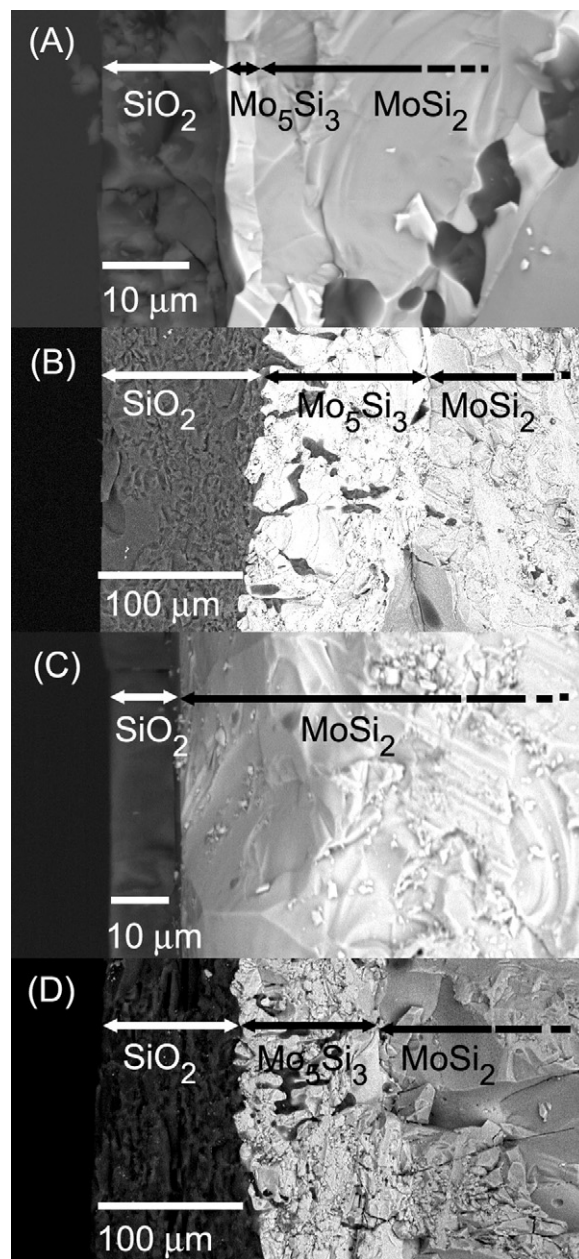


Fig. 3. Cross sections of oxide scales of (A) MoSi₂, (B) MoSi₂ + 2 at% Al, (C) MoSi₂ + 1 at% Re, and (D) MoSi₂ + 1 at% Re + 2 at% Al after isothermal oxidation at 1700 °C, for 100 h.

3 μm thick in the unalloyed sample, but its thickness was over 100 μm in Al-containing samples. There is a correlation between the thickness of the oxide and the thickness of the Mo_5Si_3 layer, as expected. As the oxide scale grows thicker, more Si is consumed, and thus a thicker Mo_5Si_3 layer is formed. Both Al-containing samples have oxide scale thickness of $\sim 100 \mu\text{m}$ and a corresponding Mo_5Si_3 layer of about the same thickness. The thickness of the oxide scale on the unalloyed and the Re-containing samples was in the range of 12–15 μm , nearly one order of magnitude less than the Al-alloyed samples. Al-alloying accelerates the oxidation rate of MoSi_2 , whereas Re-alloying does not show a significant influence.

Internal oxidation was observed in all samples; however, its extent was much greater in the samples that were alloyed with Al. In contrast to other samples, it also appears that the oxide scales on Al-containing samples were porous. It is not clear if Al-alloying makes the alloy porous, which produces a porous scale upon oxidation, or whether a porous scale grows on non-porous MoSi_2 in the presence of Al. A relatively large number of Al-containing samples should be oxidized to investigate the relationship between scale porosity and Al content.

Results of isothermal oxidation of MoSi_2 and its alloys are shown in Fig. 4 at (a) 1400 °C, (b) 1550 °C, and (c) 1700 °C. The upper case letters in the graphs of Fig. 4 correspond to the same alloy designations depicted in Fig. 3, i.e., (A) unalloyed MoSi_2 , (B) $\text{MoSi}_2 + 2 \text{ at\% Al}$, (C) $\text{MoSi}_2 + 1 \text{ at\% Re}$, and (D) $\text{MoSi}_2 + 1 \text{ at\% Re} + 2 \text{ at\% Al}$. At all the three temperatures, oxidation of unalloyed MoSi_2 , like all SiO_2 -forming materials, starts with a rapid linear rate and follows a slow parabolic rate after a stable oxide scale covers the sample. The activation energy for oxidation of MoSi_2 at this temperature range, 204 kJ/mol [19], is markedly lower than the activation energy of 340 kJ/mol reported for oxidation of MoSi_2 below 1500 °C [24]. At higher temperatures, the increase in the oxidation rates has been attributed to the enhanced diffusion of O_2 through the oxide layer as a result of transformation of amorphous SiO_2 into β -cristobalite [19]. The enhanced ordering of SiO_4^{4-} tetrahedra in β -cristobalite may allow for easier diffusion of O_2 molecules.

Different results have been reported on the effects of alloying with Al on high-temperature oxidation of MoSi_2 [14–16,25,26]. Varying amounts of Al, as well as the effects of Al-alloying on oxidation of MoSi_2 at different temperatures, produce different results. Al-alloying enhances pest oxidation resistance at low temperatures [25,27,28], but it accelerates oxidation at high temperatures [13,14,29]. Mitra and Rao [15] reported an increased oxidation rate of MoSi_2 in the presence of 2.8, 5.5, and 9 at% Al. They noted that 5.5 and 9 at% Al-containing samples had a better oxidation resistance than the 2.8 at% Al-containing sample. This was attributed to the formation of an Al_2O_3 scale on samples containing larger fraction of Al, compared to the formation of the mixture of SiO_2 and Al_2O_3 on the 2.8 at% Al-containing sample. Yanagihara et al. [14] also reported an increased oxidation rate of MoSi_2 in the presence of Al at 1627 °C and 1685 °C. However, they used 10 at% Al in their investigation. They observed an enhanced scale adhesion in the presence of Al. At lower temperatures, Al alloying is shown to have beneficial effect on oxidation of MoSi_2 , enhancing its resistance to pest-disintegration [25,26]. At higher temperatures, the presence of >9 at% Al has shown to have two effects on oxidation of MoSi_2 : it improves oxide scale adhesion and it accelerates the oxidation rate [29]. When MoSi_2 is alloyed with large fraction of Al, preferential oxidation of Al results in the formation of an Al_2O_3 scale on the samples during oxidation. On the other hand, at low fractions of Al, similar to those used in this study, adequate Al is not available for Al_2O_3 scale formation. At high temperatures and low Al contents, Al^{3+} substitutes for Si^{4+} in the tetrahedral structure of SiO_4^{4-} and acts as a network modifier. Charge balance requires a vacant O^{2-} site for every two substitutional Al atoms in the solution. These vacant sites enhance O_2 diffusion through the SiO_2

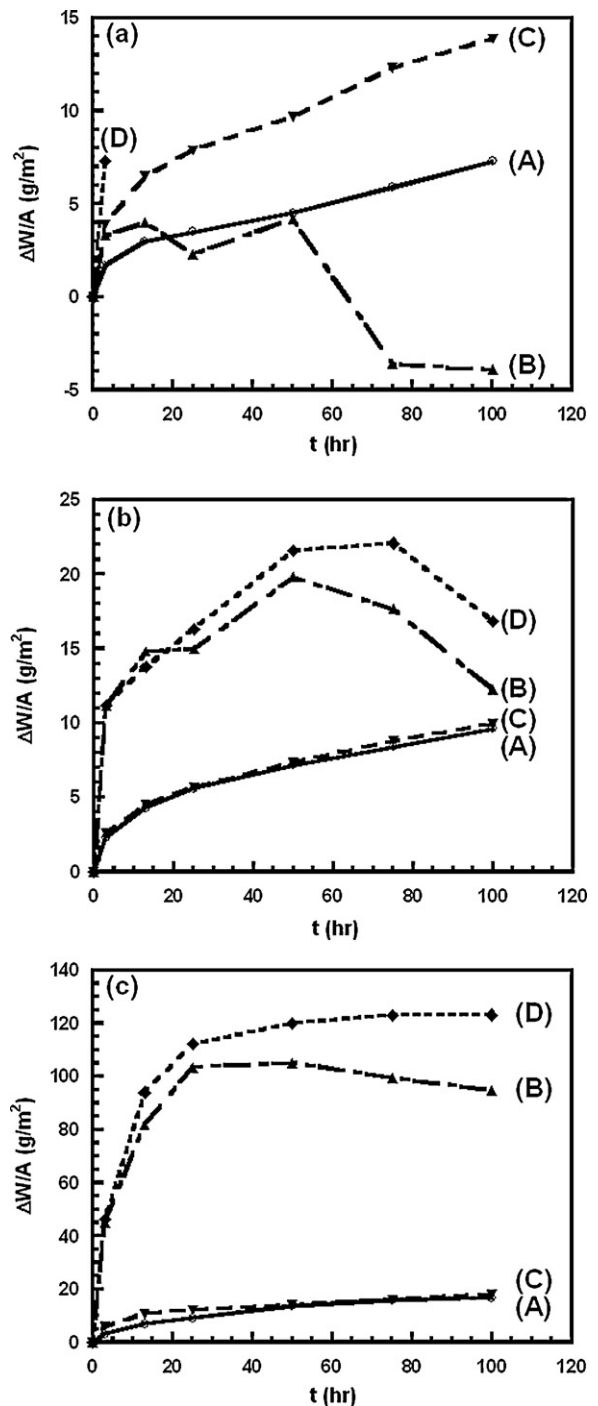


Fig. 4. Isothermal oxidation of MoSi_2 and its alloys at (A) 1400 °C, (B) 1550 °C, and (C) 1700 °C.

scale, resulting in an accelerated oxidation rate compared to the unalloyed MoSi_2 . As the thickness of the oxide layer increases, the oxide scale is no longer under plane stress. As a result, the internal stresses may cause fracture in the oxide scale, as well as severance of the scale from the sample surface, i.e., spallation. Microvoids created by vacancy defect complexes may also act as nuclei for stress concentration, facilitating the onset of fracture in the SiO_2 scale. Thus, an enhanced oxidation rate along with oxide scale spallation is observed during oxidation of 2 at% Al alloyed MoSi_2 . The initial weight gains in Al-containing samples observed in Fig. 4 result from oxidation reaction, which adds the weight of the oxygen to the samples. The weight loss at longer times is caused by spallation, as

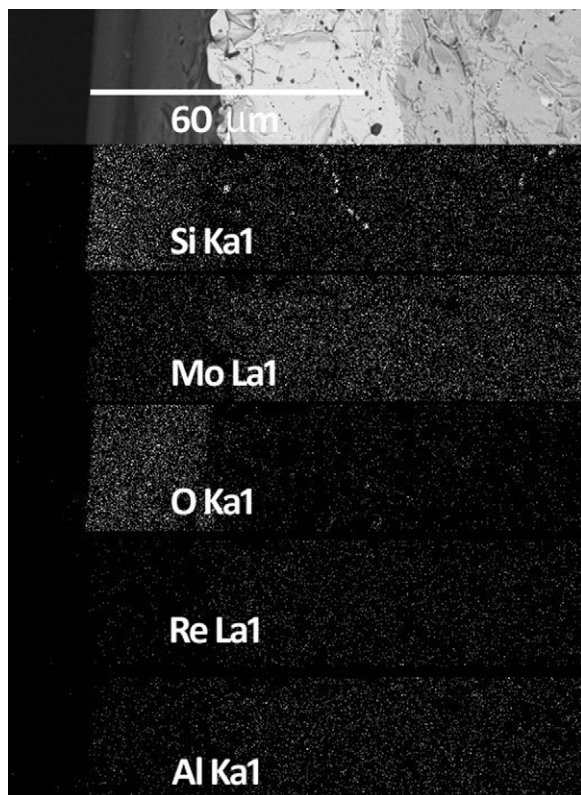


Fig. 5. Elemental dot maps of cross section of the oxide scale for MoSi₂ + 1 at% Re + 2 at% Al after isothermal oxidation at 1700 °C for 100 h.

explained. After 3 h at 1400 °C, the Al-containing sample had gained 3.3 g/m², but oxide scale spallation in the same sample caused a net weight loss after 75 h (Fig. 4a). At 1550 °C and 1700 °C, the effect of Al on oxide scale spallation was less severe. Although the oxidation rates were enhanced as shown in Fig. 4b and c, increasing temperature improved the oxide scale adhesion to the sample.

Neither Al nor Re formed oxides in any of the samples tested as shown in the dot maps of the samples for all possible elements in Fig. 5. Al and Re seem to be uniformly distributed throughout the samples. The figures also indicate that there was no preferential oxidation along the grain boundaries but evidence of selective oxidation along surface imperfections is present in Fig. 5. Re has lower affinity to oxygen than Si; therefore, Re, within the solubility limit in C11_b structure, is not expected to have significant effects on oxidation of MoSi₂. In the presence of minor amounts of Re, the formation of SiO₂ scale is expected to have rates similar to the oxidation of unalloyed MoSi₂. Experimental results indicated that 1 at% Re increased the oxidation rate of MoSi₂ at 1400 °C slightly, while at higher temperatures, Re had no effect on oxidation rate of MoSi₂, as indicated in Fig. 4b and c by specific weight gain curves that closely follow those of unalloyed MoSi₂. This is remarkable in light of the fact that Re is a very potent solution hardening element for MoSi₂.

The combined effects of 1 at% Re and 2 at% Al on oxidation of MoSi₂ is deleterious at 1400 °C. The sample exhibited a very rapid weight gain in 3 h, and it fractured into pieces soon thereafter. At higher temperatures, the Re + Al-containing samples remained in one piece, but their oxidation rates were greater than the other samples. The presence of Re enhances the deleterious effects of Al during high-temperature oxidation of MoSi₂. When Re- and Al-alloying of MoSi₂ are combined, oxidation resistance deteriorates

beyond the effects of Al-alloying alone. At 1400 °C, alloying with 2.0 at% Al resulted in oxide scale spallation, and alloying with 1 at% Re did enhance the oxidation rate, but only slightly. In contrast, alloying with 1 at% Re + 2 at% Al caused rapid weight gain and sample disintegration. At 1550 °C and 1700 °C, alloying with 1 at% Re, no remarkable effect on the oxidation of MoSi₂ could be observed. However, in the presence of Al, alloying with Re accelerates oxidation beyond the effect of Al-alloying alone. Re has low solubility in SiO₂ matrix; however, it has been shown that the presence of Al in SiO₂ enhances solubility of Re significantly [30]. The presence of Re in the oxide scale further opens the SiO₄⁴⁻ network that was already modified by Al. This results in augmenting the diffusion of O₂ molecules through the protective oxide scale, and consequently, accelerating the oxidation rate. It also degrades the adhesion of the SiO₂ scale to the bulk sample, resulting in scale spallation.

4. Conclusions

Al and Re improve low-temperature ductility and high-temperature strength of MoSi₂, respectively. Although the alloying of MoSi₂ with 2 at% Al resulted in acceleration of its oxidation rate and spallation, alloying with 1 at% Re had no remarkable effect on the oxidation of MoSi₂. However, Re has better solubility in aluminosilicate than silica. When 1 at% Re impurity was added to the alloy containing 2 at% Al, the deleterious effect of Al on oxidation of MoSi₂ was accelerated.

Acknowledgements

SEM investigations were made possible through the use of ESEM procured by National Science Foundation MRI Grant number CMS-0321226. This research was, in part, supported by the National Science Foundation CREST Grant HRD-0932421.

References

- [1] M.G. Hebsur, M.V. Nathal, Structural Intermetallics the Minerals, Metals and Materials Society, Warrendale, PA, 1997, 949.
- [2] K. Kurokawa, H. Houzumi, I. Saeki, H. Takahashi, Mater. Sci. Eng. A261 (1999) 292–299.
- [3] A.A. Sharif, A. Misra, T.E. Mitchell, Scripta Mater. 52 (2005) 399–402.
- [4] H. Inui, K. Ishikawa, M. Yamaguchi, Intermetallics 8 (2000) 1131–1145.
- [5] K. Peng, M. Yi, L. Ran, Y. Ge, Mater. Chem. Phys. 129 (2011) 990–994.
- [6] K. Hagihara, T. Nakano, Acta Mater. 59 (2011) 4168–4176.
- [7] T. Dasgupta, A.M. Umarji, Intermetallics 16 (2008) 739–744.
- [8] U.V. Waghmare, V.V. Bulatov, E. Kaxiras, M.S. Duesbery, Mater. Sci. Eng. A 261 (1999) 147–157.
- [9] H. Inui, M. Moriwaki, K. Ito, M. Yamaguchi, Philos. Mag. A 77 (1998) 375–394.
- [10] H. Inui, T. Nakamoto, K. Ishikawa, M. Yamaguchi, Mater. Sci. Eng. A 261 (1999) 131–138.
- [11] Y. Harada, Y. Murata, M. Morinaga, Intermetallics 6 (1998) 529–535.
- [12] A.A. Sharif, A. Misra, J.J. Petrovic, T.E. Mitchell, Scripta Mater. 44 (2001) 879–884.
- [13] T. Maruyama, K. Yanagihara, K. Nagata, Corros. Sci. 35 (1993) 939–944.
- [14] K. Yanagihara, T. Maruyama, K. Nagata, Intermetallics 3 (1995) 243–251.
- [15] R. Mitra, V.V.R. Rao, Mater. Sci. Eng. A 260 (1999) 146–160.
- [16] P.S. Kisly, V.U. Kodash, V.J. Shemet, High Temp. Sci. 28 (1989) 379–383.
- [17] S. Knittel, S. Mathieu, M. Vilasi, Intermetallics 18 (2010) 2267–2274.
- [18] S. Knittel, S. Mathieu, M. Vilasi, Intermetallics 19 (2011) 1207–1215.
- [19] A.A. Sharif, J. Mater. Sci. 45 (2009) 865–870.
- [20] R.L. Fleischer, Acta Metall. 11 (1963) 203–209.
- [21] A. Misra, F. Chu, T.E. Mitchell, Philos. Mag. A 79 (1999) 1411–1422.
- [22] S.A. Maloy, A.H. Heuer, J.J. Lewandowski, T.E. Mitchell, Acta Metall. Mater. 40 (1992) 3159–3165.
- [23] L.A. Cornish, M.J. Witcomb, J. Alloys Compd. 291 (1999) 117–129.
- [24] C.D. Wirkus, D.R. Wilder, J. Am. Ceram. Soc. 49 (1966) 173–177.
- [25] A. Stergiou, P. Tsakiroopoulos, Struct. Intermetallics (1997) 869–875.
- [26] A. Stergiou, P. Tsakiroopoulos, A. Brown, Intermetallics 5 (1997) 69–81.
- [27] K. Yanagihara, T. Maruyama, K. Nagata, Intermetallics 4 (1996) S133–S139.
- [28] K. Yanagihara, K. Przybylski, T. Maruyama, Oxid. Met. 47 (1997) 277–294.
- [29] T. Maruyama, K. Yanagihara, Mater. Sci. Eng. A 239–240 (1997) 828–841.
- [30] J. Nilsson, J. Laegsgaard, A. Bjarklev, Optical Amplifiers, 1st ed., Taylor & Francis, Boca Raton, FL, 2006, 559.